International Conference on Lightning Protection
33rd International Conference on Lightning Protection
25 - 30 September 2016
Estoril, Portugal

Small- and large-current cloud-to-ground lightning over southern China

Dong Zheng, Yijun Zhang, Qing Meng
State Key Laboratory of Severe Weather
Chinese Academy of Meteorological Sciences
Beijing, China
zhd@camscma.cn

Luwen Chen
Lightning Protection Center of Guangdong Province
Guangzhou, Beijing

Abstract*—The first climatological comparison of small-current cloud-to-ground (SCCG; peak current ≤ 50 kA) and large-current cloud-to-ground (LCCG; peak current > 50 kA, > 75 kA, and > 100 kA) lightning flashes is presented for South China. The percentage of positive LCCG lightning during the non-rainy season was more than twice that during the rainy season, while the percentage of positive SCCG showed small seasonal differences. A positive cloud-to-ground (PCG) lightning was more likely to feature a large peak current than a negative cloud-to-ground (NCG) lightning, especially during the non-rainy season and over land. Distinct geographical differences are found between SCCG and LCCG lightning density and between their own positive and negative discharges. Furthermore, the percentages of positive lightning in LCCG and SCCG lightning exhibit distinctly different geographical and seasonal (rain and non-rainy season) distributions. The diurnal variations in SCCG and LCCG lightning are clearly different over sea but similar over land. Diurnal variations in the percentage of positive lightning are functions of the peak current and underlying surface. In combination with the University of Utah precipitation feature (PF) dataset, it is revealed that thunderstorms with relatively weak convection and large precipitation areas are more likely to produce the LCCG lightning, and the positive LCCG lightning is well related with mesoscale convective systems in the spatial distribution during non-rainy season.

Keywords-lightning; small and large peak currrent; Climatological Comparision

I. INTRODUCTION

The climatology of lightning flashes has been widely studied around the world. These studies have investigated the geographical distribution and seasonal and diurnal variability of lightning activities generally using lightning data as a whole. Thus, the question remains whether cloud-to-ground (CG) lightning flashes with different peak-current magnitudes have different climatological characteristics.

Special attention has been paid to large-current CG (LCCG) lightning in several previous studies [1–3]. In these studies, LCCG lightning is usually defined as having peak current higher than 75 kA [1, 3] or 100 kA [2]. These studies have revealed distinct geographical differences in the spatial distribution of positive and negative LCCG lightning. It has been proposed that positive LCCG lightning density distribution were related to the occurrence of mesoscale convective systems (MCSs) [1, 3]. Furthermore, it was reported that PCG lightning accounts for a relatively higher proportion of LCCG lightning than for total CG lightning.

In this paper, we focus on the climatological differences between small-current CG (SCCG) and LCCG lightning by analyzing CG lightning data in southern China, mainly in Guangdong province and its adjacent sea. We further compare SCCG and LCCG lightning across seasons (rainy and non-rainy seasons) and underlying surfaces (land and offshore water), and discuss the association of LCCG lightning with intensity of thunderstorms and association of positive LCCG lightning with MCSs.

II. OBSERVATIONS AND DATA

A. *Study Area*

The study region (Fig. 1) has a total area of approximately 244,000 km^2, including the land within Guangdong Province, southern China (approximately 180,000 km^2), and an adjacent stretch of the South China Sea (64,000 km^2). The seaward extent of the study region was limited to approximately 100 km from the coastline to ensure reliable detection by the lightning location system.

B. *Observational Data and Processing*

CG lightning data are collected by the Guangdong Lightning Location System (GDLLS) operated by the State Grid Electric Power Research Institute. This system began operation in 1996 and, by 2000, comprised a network of 16 time-of-arrival/magnetic direction finder sensors (Fig. 1). From 2007 to 2010, the system was further upgraded and the number of sensors increased to 27 (Fig. 1). According to the study on the performance of GDLLS [4], the lightning detection efficiency and stroke detection efficiency were about 94% and 60%, respectively, the median values for location error were approximately 489 m, and the median absolute percentage errors of peak current estimation were about 19.1%. GDLLS data from 2001 to 2013 are used for this study.

Original return stroke (RS) data were grouped using the criterion that adjacently located RSs for one lightning flash should occur within an interval of 0.5 s and a distance of 10 km. Furthermore, the maximum peak current among the RSs was taken to be the lightning current. PCG lightning with current less than 10 kA was removed from the dataset because it could be misinterpreted as cloud lightning [5]. CG lightning flashes were divided into two categories: lightning with a peak current no larger than 50 kA was defined as SCCG lightning, and that with a peak current above 50 kA was defined as LCCG lightning. The latter category was further split into three types: CG lightning with peak current above 50, 75, and 100 kA, hereafter referred to as CG50, CG75, and CG100 lightning, respectively. We will mainly focus on CG75 lightning, as this was the definition of LCCG lightning used in previous studies [1, 3].

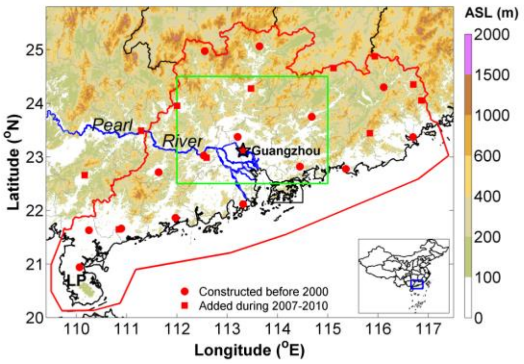

Figure 1. Study region (delineated by red line) in Guangdong Province and adjacent coastal waters, with the inset map showing the location of the study region within China. Red dots and squares mark the position of the sensors of (GDLLS) constructed during different periods. Leizhou Peninsula is labeled as 'LP'. The green rectangle shows the region discussed in Section 4.

A total of more than 23 million CG lightning flashes were detected within the analysis region between 2001 and 2013. In the analysis on geographic distribution of the lightning features, the values were counted in 0.5 °resolution grids.

The University of Utah TRMM-based (TRMM: Tropical Rainfall Measuring Mission satellite) precipitation feature (PF) dataset [6] from 2001 to 2013 is also used in Section 4 to characterize the structure and convective properties of precipitation systems.

III. Analysis and Results

A. Overiew of the CG lightning flashes

Some basic characteristics of CG lightning data are shown in Fig. 2. Fig. 2a shows the percentages of the different CG lightning types (SCCG or LCCG lightning under different peak current thresholds) in total CG lightning. LCCG lightning was proportionately a little more frequent during the rainy season than during the non-rainy season. While the SCCG lightning was more common over land than sea, LCCG lightning was much more likely to occur over sea. In addition, the land–offshore contrast in the percentage of LCCG lightning extends with the increase of the LCCG lightning peak-current threshold.

Referring to Fig. 2b, the percentage of positive lightning was higher for LCCG lightning than SCCG lightning. Furthermore, the percentage of positive LCCG lightning increased with increasing peak-current threshold. The percentage of positive SCCG lightning shows slight differences related to both season and the underlying surface. However, the percentage of positive LCCG lightning during the non-rainy season was more than twice that during the rainy season. The land–sea contrast in the percentages of positive LCCG lightning is not as prominent as the seasonal contrast; however, the percentages were smaller over land than over sea for SCCG and CG50 lightning. This situation was reversed for CG75 and CG100 lightning.

We considered the percentage of different CG lightning types that occurred in PCG (P_{PCG}) and NCG (P_{NCG}) lightning. The ratios of P_{PCG} to P_{NCG} are shown in Fig. 2c to explore the difference of PCG or NCG lightning in contributing different CG lightning types. The percentages of LCCG lightning in PCG lightning were larger than in NCG lightning, and furthermore, this tendency increased with an increase in the peak-current threshold. For example, a PCG lightning flash was 1.5 times more likely than an NCG lightning flash to exceed 75 kA. In addition, the difference in the percentages of LCCG lightning in PCG and NCG lightning was more prominent during the non-rainy than the rainy season, and was more outstanding over land than over sea, while the LCCG lightning in PCG lightning kept larger percentage than that in NCG lightning.

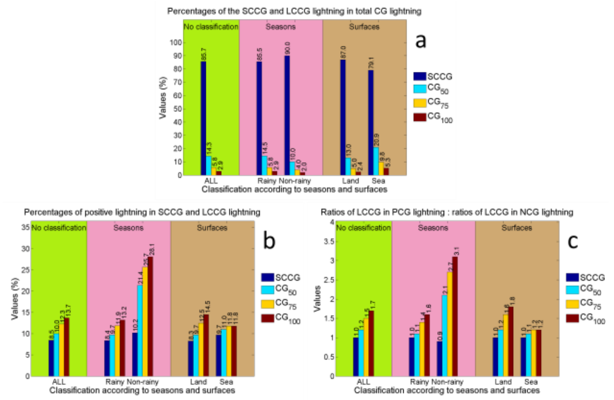

Figure 2. Basic characteristics of the SCCG and LCCG lightning for different seasons and underlying surfaces: (a) percentages of SCCG and LCCG lightning in total CG lightning; (b) percentages of PCG lightning in SCCG and LCCG lightning; (c) ratios of P_{PCG} to P_{NCG} (P_{PCG}: percentage of different CG lightning types in PCG lightning; P_{NCG}: percentage of different CG lightning types in NCG lightning).

B. Geographical Distribtuion of Lightning Density

Fig. 3a and b reveal that, during the rainy season, positive and negative SCCG lightning flashes both exhibit the highest densities in a region over the Pearl River Delta (PRD) centered on Guangzhou City and the secondary high-density regions to the north of the Leizhou Peninsula (LP). The density along the coastline decreased sharply from land towards sea.

Interestingly, the distributions of positive and negative SCCG lightning varied during the non-rainy season (Fig. 3c and d) and were entirely different from the patterns of their counterparts during the rainy season. Compared to that the highest densities of both positive and negative were located over PRD during rainy season (Fig. 3a and b), during the non-rainy season, the highest density of positive SCCG lightning generally occurred along the central coastline in the study region (Fig. 3c), and that of negative SCCG lightning was distributed across the mid-west part of the study region (Fig. 3d).

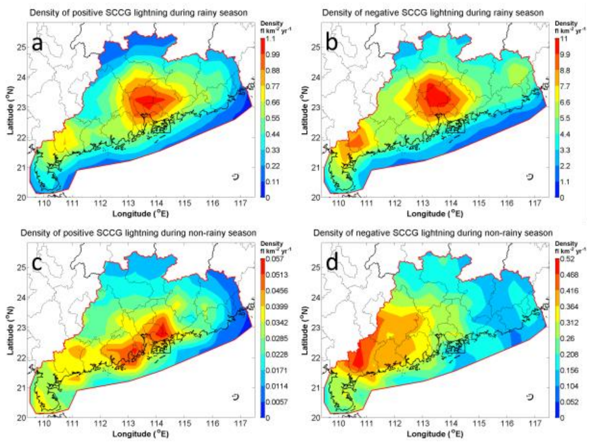

Figure 3. Distribution of (a) positive and (b) negative SCCG lightning during the rainy season, and during the non-rainy season ((c) and (d), respectively).

Fig. 4 shows the density distributions of positive and negative CG_{75} lightning during the two seasons. The spatial distributions of the CG_{50} and CG_{100} lightning were qualitatively similar, and are therefore not shown. The distributions of LCCG and SCCG lightning showed geographical differences during the two seasons. During the rainy season, the positive and negative LCCG lightning both had the high density centers over the PRD (Fig. 4a and b); however, their locations were more inclined to the mouth of the Pearl River, compared to those of positive and negative SCCG lightning during the same season. The positive LCCG lightning had another high density center to the north of LP, where the negative LCCG lightning was not prominent in density.

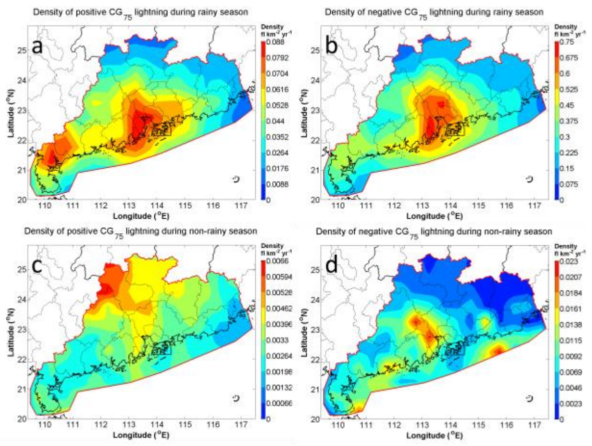

Figure 4. As Fig. 3, but for positive and negative CG_{75} lightning.

During the non-rainy season, the highest density of positive LCCG lightning was mainly found over mountainous areas to the north of the analysis region (Fig. 4c). The highest density of negative LCCG lightning, however, occurred in the west of PRD, with some large densities scattering in some other isolated centers (Fig. 4d).

C. Geographical Distribution of Positive Lightning in SCCG and LCCG lightning

Fig. 5 shows the geographical distributions of PCG lightning ratios in different CG lightning types during the rainy and non-rainy seasons. According to Fig. 5a and b, the ratios of positive SCCG lightning to total SCCG lightning during rainy and non-rainy seasons have analogous spatial patterns, with greater values near the mouth of the Pearl River and extend to the east pat of study region. But during the rainy season, the positive SCCG ratios distributed more continuously in space, and during the non-rainy season, the largest positive SCCG ratios was located in the east of the study region. The ratios of positive LCCG lightning (Fig. 5c and d), however, showed different spatial distributions to the ratios of positive SCCG lightning during all seasons. Furthermore, the ratio of positive LCCG lightning had different spatial patterns during different seasons. During the rainy season (Fig. 5c), areas with large positive LCCG lightning ratios were mainly located to the north of LP, while the PRD featured small values. During the non-rainy season (Fig. 5d), larger positive LCCG ratios were distributed in the north and northeast parts of the analysis region.

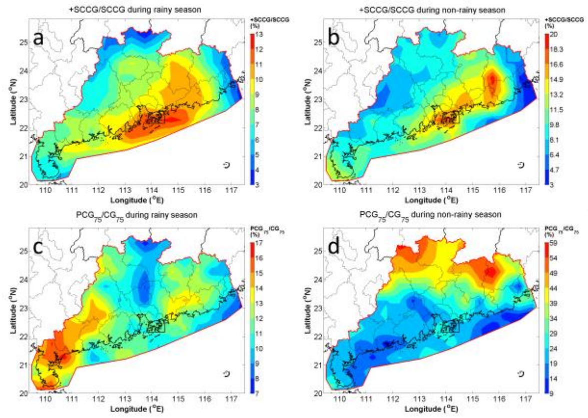

Figure 5. Geographical distributions of percentages of positive lightning in different CG lightning types: (a) ratio of positive SCCG lightning to total SCCG lightning during the rainy season; (b) same as (a) but during the non-rainy season; (c) ratio of positive CG_{75} lightning to total CG_{75} lightning during the rainy season; and (d) same as (c) but during the non-rainy season.

D. Diurnal Variation

Fig. 6 shows diurnal variations in CG lightning activity based on all data in both rainy and non-rainy seasons. We use CG_{75} lightning data to represent LCCG lightning. Diurnal variations in the CG_{50} and CG_{100} lightning are similar to those for CG_{75} lightning and are not shown.

Diurnal variations in the SCCG and LCCG lightning (Fig. 6a) exhibit a clear dependence on the underlying surface. Both SCCG and LCCG lightning flashes over land reached a peak at 1600 LT (local time; indicating the period 1600–1700 LT), and a minimum at 0900 and 1000 LT, respectively. SCCG and LCCG lightning flashes over sea both had two peaks. For the SCCG lightning, the main peak occurred at 1700 LT and the second peak occurred at 0500 LT. In contrast, CG_{75} lightning had a main peak at 0700 LT and a second peak at 1800 LT. The CG_{50} and CG_{100} flashes also had main peaks in the morning and secondary peaks in the afternoon. Furthermore, we calculated the main-peak densities of LCCG lightning are 1.1, 1.3 and 1.5 times the second-peak densities for the CG_{50}, CG_{75}, and CG_{100} lightning, respectively, which suggests that the main morning LCCG lightning peak changed more noticeably with an increase in peak-current threshold. Note that, from 2100 to 1100 LT, the LCCG lightning density over sea was even higher than over land. Meanwhile, the SCCG lightning from 2100 to 1100 LT was of similar density over land and sea.

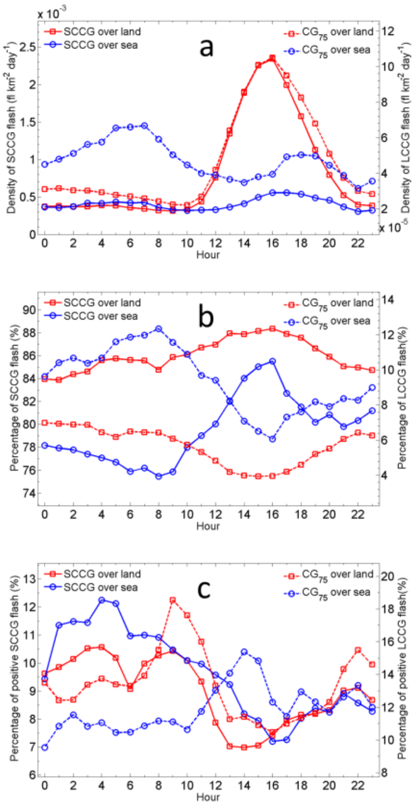

Figure 6. Diurnal variations in: (a) the density of different CG lightning types, (b) the percentages of different CG lightning types in total CG lightning, and (c) the percentages of the positive lightning in different CG lightning types.

Fig. 6b shows the diurnal variation in percentages of SCCG and LCCG lightning to the total CG lightning. SCCG lightning occurred more frequently in the afternoon with the peaks at 1600 LT over both land and sea; the percentage of CG_{75} lightning over land was highest at 0000 LT, while the percentage of CG_{75} lightning over sea peaked at 0800 LT. It is apparent that diurnal variations in the percentage of LCCG lightning have an inverse relationship with solar heating.

In terms of the percentages of positive lightning in different CG lightning types (Fig. 6c), the percentage of positive SCCG lightning peaked in the morning and was lowest in the afternoon, over both land and sea. However, the peak percentage of positive CG_{75} lightning depended on the underlying surface. The percentage of positive CG_{75} lightning over land peaked at 0900 LT, and was lowest at 1600 LT. The percentage of positive CG_{75} lightning over sea, however, peaked at 1400 LT, and reached the minimum at 0000 LT. The percentages of positive CG_{50} and CG_{100} lightning were similar, except for a negligible difference in the times of the maxima and minima. The ratios of the highest to lowest percentages for CG_{50}, CG_{75}, and CG_{100} lightning were 2.1, 1.8, and 1.5, respectively, over land, and 1.4, 1.6, and 1.9, respectively, over sea. Therefore, diurnal fluctuations in positive LCCG lightning ratios decreased over land and increased over sea with an increase in peak-current threshold.

IV. Discussion

The analysis in this study has exposed distinct differences between the properties of SCCG and LCCG lightning and their spatial and temporal distribution. Previous studies have suggested some mechanisms to explain the larger peak current of lightning over sea than over land [3, 7, 8]. Here, we will focus on another mechanism associated with intensity of thunderstorm to illustrate the diurnal variation of the percentage of LCCG lightning.

A. *Mechanism associated with thunderstorm*

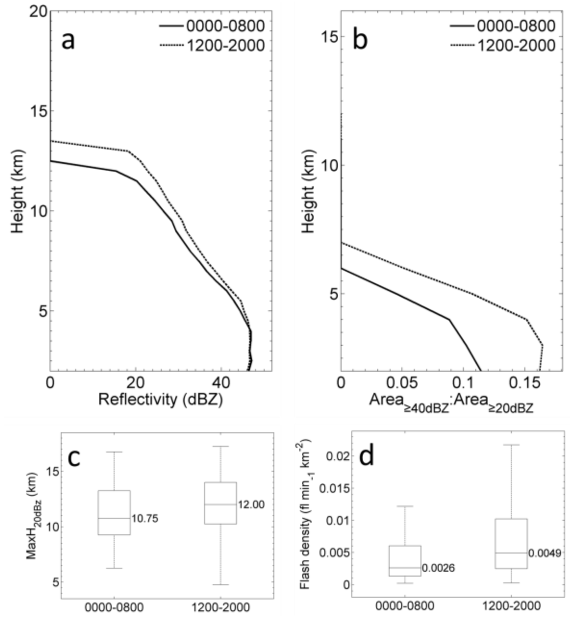

Figure 7. Comparison of convection intensity proxies and precipitation features during 0000−0800 LT and 1200−2000 LT: (a) maximum reflectivity with height; (b) ratio of ≥40 dBZ area to ≥20 dBZ areas with height; (c) box-and-whisker plot for maximum height of the 20-dBZ echo; and (d) box-and-whisker plot for flash density relative to convective area (the LIS flash count was divided by view time and then divided by convection area).

Chronis [9] and Chronis et al. [10] elaborated on the possible relationship between lightning peak currents and thunderstorms. To put it simply, thunderstorms with stronger updrafts and more intense electrification have a reduced breakdown electric field because of the greater concentration of charged hydrometeors [11], and tend to feature pockets of opposite charge closer together because of the more turbulent mixing. This would cause more frequent lightning initiation and discharges, but less available charge for neutralization of the RS, which would result in a small peak current. In contrast, for relatively weak thunderstorms, the larger charge centers and thundercloud fields support larger peak current yields but low lightning frequency.

By using TRMM PF data to investigate the structure of precipitation systems with lightning discharge, we then examine the possible association of large peak currents with convection intensity. In order to exclude the impact of the underlying surface, we fix the analysis area to a rectangular region over land (shown in Fig. 1) that includes the zone with most frequent lightning flashes. Two analysis intervals are chosen: from 0000 to 0800 LT when the ratio of LCCG lightning to the CG lightning is large over land, and from 1200 to 2000 LT when the ratio is small over land (see Fig. 6b). A total of 100 PFs from 0000 to 0800 LT and 360 PFs from 1200 to 2000 LT were ultimately obtained in the region. Four proxies are chosen to express the PF convection intensity: vertical profiles of maximum reflectivity, vertical profiles of the ratio of ≥40 dBZ area to ≥20 dBZ areas (for investigating the height distribution of the convective component in total precipitation), maximum height of the 20-dBZ echo, and flash density relative to the convection area. The comparison of these proxies during the two time intervals is shown in Fig. 7.

All proxies in Fig. 7 suggest that the thunderstorms during 1200−2000 LT generally featured stronger convection than those during 0000−0800 LT. In addition, Fig. 7d further indicates that, for the same convection area, storms during 1200−2000 LT were more likely to produce larger number of lightning flashes than those during 0000−0800 LT. These results, combined with the diurnal variation in LCCG lightning ratios (Fig. 6b), proposed that relatively weak storms tended to produce higher percentage of LCCG lightning, while strong storms tended to produce more frequent lightning discharge but a lower percentage of LCCG lightning. The results shown in Fig. 7d may support the concept of pocket charges in storms with strong convection, i.e., stronger convection trends to result in more pocket charges that cause more frequent lightning activity in per unit area.

Fig. 8 shows the precipitation region area (Fig. 8a) and ratio of the stratiform to precipitation areas (Fig. 8b) during 0000−0800 LT and 1200−2000 LT, respectively. Thunderstorms during 0000−0800 LT were more likely to have greater average horizontal extensions and stratiform regions. Large cloud areas, and especially large stratiform areas, might contribute to horizontal spreading of the charge, and hence to the formation of large horizontally orientated charge regions featuring long-propagation lightning flashes. According to [10], a continuous charge over a large area might cause large thundercloud fields and large peak currents per CG while the CG frequency is low. This suggestion is supported by new work ("unpublished" [12]). Based on 10 MCSs, they found that median peak currents in the first RS in the stratiform region were 26% and 24% greater than their counterparts in the convective region. Therefore, Fig. 7 and 8 proposed that the thunderstorms with relatively weak convection and large precipitation size are more likely to produce LCCG lightning.

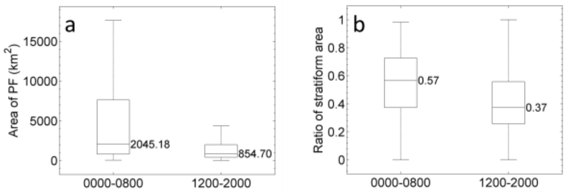

Figure 8. Precipitation area from TRMM/PR, and (b) ratio of stratiform to total precipitation area.

B. Associated between Positive LCCG Lightning and MCSs

Because the ratio of positive LCCG lightning is high during 0000−0800 LT (although the peak was at 0900 LT) and low during 1200−2000 LT (See Fig. 6c), Fig. 7 and 8 also suggest a relationship between positive LCCG lightning and large-area thunderstorms from the perspective of diurnal variations in lightning activity.

Next, we examine the association between geographical patterns during different seasons. PFs accompanied by LIS flash records and with areas larger than 1000 km^2 were considered as MCS-type PFs, and those accompanied with lightning with an area smaller than 1000 km^2 were considered as sub-MCS-type PFs.

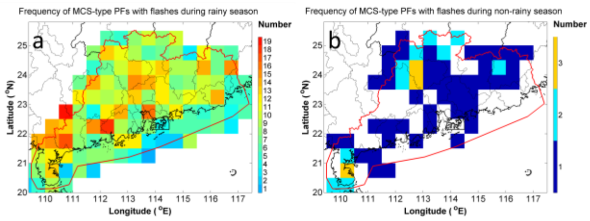

Figure 9. FGeographical distributions of MCS-type PFs with flashes during (a) the rainy season, and (b) the non-rainy season.

Fig. 9 shows the geographical distribution of the frequency of MCS-type PFs over the study region during the rainy (Fig. 9a) and non-rainy seasons (Fig. 9b), with the frequency being calculated from grid sizes of 0.5°. Comparing Fig. 9a with Fig. 4a, it looks that the spatial association between the high density of positive LCCG lightning and the high-frequency MCS-type PFs was weak during the rainy season. But, there is a more distinct relationship between positive LCCG lightning and MCS-type PFs during the non-rainy season. In this season, an area of high-frequency MCS-type PFs was located to the north of the analysis region (Fig. 9b) where there was also a high density of positive LCCG lightning (Fig. 4c) and large ratio of positive LCCG lightning (Fig. 5d). At the same time, there was no apparent spatial correspondence between MCS-type PFs and positive SCCG lightning (refer to Fig. 3c and Fig. 5b) and between MCS-type PFs and negative LCCG lightning (Fig. 4d).

Hence, the analysis suggests a positive relationship between positive LCCG lightning and MCSs, especially during the non-rainy season.

V. CONCLUSIONS

In this paper, we produce the first climatological comparison of SCCG and LCCG lightning over southern China. Our results show a distinct contrast between the properties of SCCG lightning and LCCG lightning, and their geographical distribution and diurnal variation. These properties change with season and also depend on the underlying surface.

The percentage of LCCG lightning in total CG lightning was much greater over sea than over land. Relative to SCCG lightning, LCCG lightning was slightly more likely to be positive. Furthermore, the percentage of positive LCCG lightning during the non-rainy season was more than twice that during the rainy season. However, the percentage of positive SCCG lightning showed only small seasonal differences. A PCG lightning flash was more likely to feature a large peak current than a NCG lightning flash, especially during the non-rainy season and over land. Meanwhile, the percentages of SCCG lightning in PCG and NCG lightning were similar.

There were distinct geographical differences between SCCG and LCCG lightning densities, and between the density distribution of positive and negative discharges within these types. The geographical distribution of the same-type or same-polarity CG lightning was different for rainy and non-rainy seasons. The geographical distributions of the ratio of PCG lightning in SCCG lightning were roughly similar in the rainy and non-rainy seasons, whereas the ratios of PCG lightning in LCCG lightning exhibited distinctly different geographical distributions from those in SCCG lightning, and also differed between rainy and non-rainy seasons.

In terms of diurnal variations, SCCG and LCCG lightning flashes over land both peaked at 1600 LT, while those over sea had two peaks: one in the morning and the other in the afternoon. However, the main peak in SCCG lightning occurred in the afternoon, while the main peak for LCCG lightning occurred in the morning. This caused a larger LCCG lightning ratio in the morning than in the afternoon. On the other hand, the percentage of positive SCCG lightning peaked in the morning, and was lowest in the afternoon over both land and sea. However, the percentage of positive LCCG lightning had a morning peak over land and an afternoon peak over sea. Furthermore, with the increase in the peak-current threshold, the diurnal fluctuations in the percentage of positive LCCG lightning decreased over land but increased over sea.

In terms of diurnal variations of LCCG lightning and structures of TRMM PFs with LIS flash observation, it was found that thunderstorms with relatively weak convection and large precipitation areas were more likely to produce LCCG lightning. Furthermore, active positive LCCG lightning was associated with large-area MCS-type PFs, and this was particularly evident in the spatial distribution during the non-rainy season. This might be attributed to the preference of positive LCCG lightning in the stratiform regions of MCSs.

ACKNOWLEDGMENT

This work is supported by Basic Research Fund of Chinese Academy of Meteorological Sciences (Grant No. 2014R017) and Natural Science Foundation of China (41405004).

REFERENCES

[1] W. A. Lyons, M. Uliasz and T. E. Nelson, “Larege Peak current cloud-to-ground lightning flashes during the summer months in the Contiguous United States,” Mon. Wea. Rev., vol. 126, 1998, pp. 2217–2233.

[2] B. Kochtubajda, W. R. Burrows, and B. E. Power, “Large current lightning flashes in Canada,” Proc. 2nd Conf. on Meteorological Applications of Lightning Data, P2.11, Atlanta, Georgia, USA, AMS, 2006.

[3] O. Jr. Pinto, I. R. C. A. Pinto, D. R. de Campos, and K. P. Naccarato, “Climatology of large peak current cloud-to-ground lightning flashes in southeastern Brazil,” J. Geophys. Res., vol. 114, D16105, 2009, doi:10.1029/2009JD012029.

[4] L. Chen, et al., “Performance Evaluation for a Lightning Location System Based on Observations of Artificially Triggered Lightning and Natural Lightning Flashes,” J. Atmos. Oceanic Technol., vol. 29, 2012, pp. 1835–1844.

[5] K. L. Cummins, et al., “A combined TOA/MDF technology upgrade of the U.S. National Lightning Detection Network,” J. Geophys. Res., vol. 103, 1995, pp. 9035–9044.

[6] C. Liu, “University of Utah TRMM precipitation and cloud feature database: Description version 1.0,” University of Utah Department of Meteorology , 2007, [available online at http://trmm.chpc.utah.edu/docs/trmm_database_description_v1.0.pdf.]

[7] L. J. Tyahla, and R. E. Lopez, “Effect of surface conductivity on the peak magnetic field radiated by first return strokes in cloud-to-ground lightning,” J. Geophys. Res., vol.99, 1994, pp.10517−10525.

[8] K. L. Cummins, J. A. Cramer, W. A. Brooks, and E. P. Krider, “On the effect of land-sea and other earth surface discontinuities on LLS-inferred lightning parameters,” Proc. 8th Int. Symp. on Lightning Protection, pp. 106–111, 21–25 November, São Paulo, Brazil, 2005.

[9] T. G. Chronis, “Preliminary lightning observations over Greece,” J. Geophys. Res., vol.117, D03113, 2012, doi:10.1029/2011JD017063.

[10] T. Chronis, et al., “Climatological diurnal variation of negative CG lightning peak current over the continental United States,” J. Geophys. Res. Atmos., vol.120, 2015, pp.582−589, doi:10.1002/2014JD022547.

[11] D. Petersen, M. Bailey, W. H. Beasley, and J. Hallett, “A brief review of the problem of lightning initiation and a hypothesis of initial lightning leader formation,” J. Geophys. Res., vol.113, D17205, 2008, doi:10.1029/2007JD009036.

[12] F. Wang, Y. Zhang, H. Liu, W. Yao, and Q. Meng, “Characteristics of cloud-to-ground lightning strikes over the stratiform region of mesoscale convective system,” Submitted to Atmos. Res., in review.